

**UNDERSTANDING REGOLITH DISTRIBUTION ON 433 EROS USING ANALYSES OF PIT CHAINS AND GROOVES.** D.Y. Wyrick<sup>1</sup> and D.L. Buczowski<sup>2</sup>, <sup>1</sup>Dept. of Earth, Material, and Planetary Sciences, Southwest Research Institute®, 6220 Culebra Road, San Antonio, TX 78238-5166, dwyrick@swri.org, <sup>2</sup>Planetary Exploration Group, Johns Hopkins University Applied Physics Lab, Laurel, MD 20723, Debra.Buczowski@jhuapl.edu.

**Introduction:** From 2000 to 2001 the Near-Earth Asteroid Rendezvous NEAR-Shoemaker spacecraft orbited the asteroid 433Eros. Tens of thousands of high resolution images were collected in that year by the NEAR Multi-Spectral Imager (MSI). These images revealed that Eros is criss-crossed by hundreds of lineations, including both extensional and contractional features. A global database of all Eros lineaments has been created to better understand the global distribution of these features [1]. Extensional lineations provide additional clues to the underlying structure of the asteroid and the spatial distribution of regolith thickness.

Extensional lineations range from pits to grooves to fractures; this range of morphologies is likely a function of underlying fracture dilation, regolith thickness, and the mechanical properties of the regolith. Grooves and pit chains have been identified on Eros [2] (Fig. 1), as well as other small bodies such as Phobos [3], Gaspra [4], and Ida [5].

Grooves and pit chains on Eros have been interpreted to form by collapse of surface regolith into underlying fractures [3, 4], consistent with hypotheses

for similar features on Mars [6, 7] and Earth [8]. Regolith thickness and its mechanical properties likely play a significant role in pit chain size and morphology [7]. The grooves observed by [2] have been mapped as part of a set of similarly oriented lineations in the southern hemisphere [1, 9], located between the southern lip of Shoemaker Regio and the south pole (Fig. 2). When compared to the volume of low-velocity ejecta from Shoemaker crater [10], it is observed that pit chains occur only where the lineation set overlaps the region of thickest regolith [11], as predicted by [2].

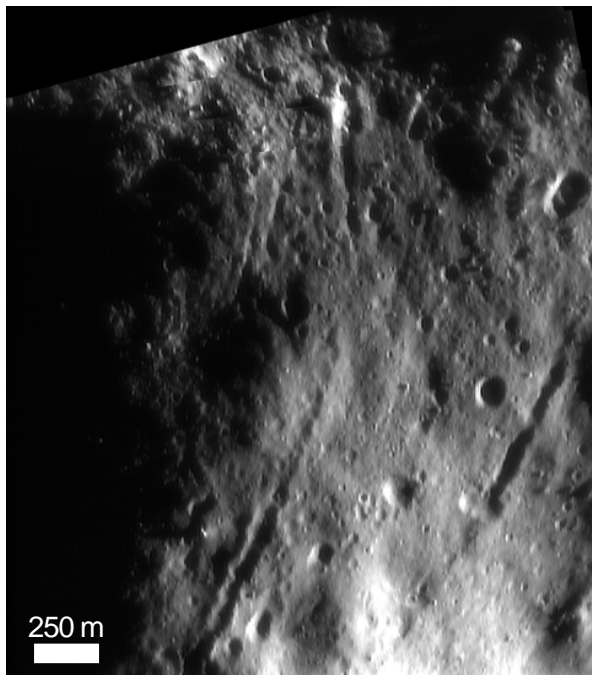


Figure 1. Mosaic of Eros images 135344864 - 135345560, showing scalloped grooves with the morphology of merged pits, as observed by [2]. Mosaic is centered at approximately 54°S, 316°W.

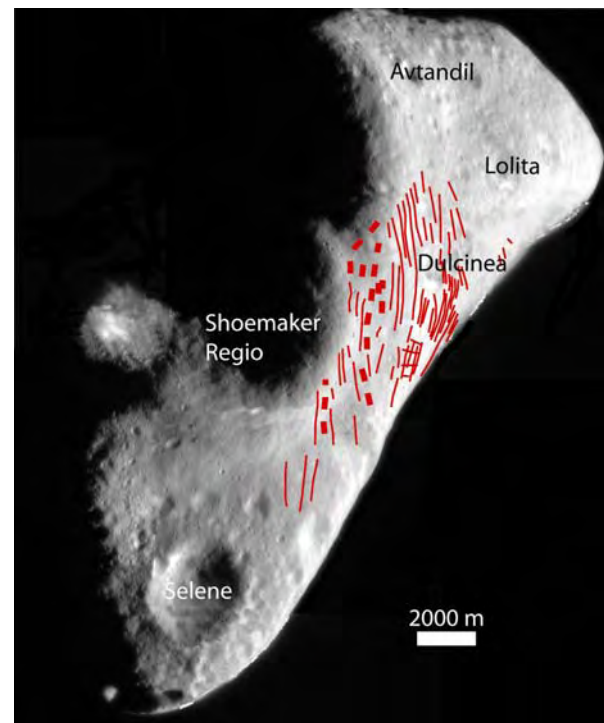


Figure 2. Eros southern hemisphere mosaic, made up of images 151025658 - 151026340, showing one group of similarly oriented lineations from the global map. Dashed lines indicate lineations that are pit chains.

**Analysis:** Determining the range of groove and pit chain size, slope and volume will provide data to constrain the regolith properties necessary to produce these features. Building on the previous work of [12] and [2], detailed morphometric analyses of grooves, pits and pit chains are being performed to determine (i) pit/groove diameter and depths; (ii) pit/groove volume; (iii) pit/groove slope; and (iv) along-strike variation in

these values. These calculations will follow the detailed methodology outlined in [7]. Measurements of pit diameter and shadow length on registered and projected images, along with sun inclination and azimuth, can be used to calculate the slope and depth of the pit. Volumes can then be calculated using shadow morphology to determine the pit geometry. These data can then be used to determine the minimum volume of subsurface fracture dilation required to accommodate downward drainage of material for formation of pit chains and grooves.

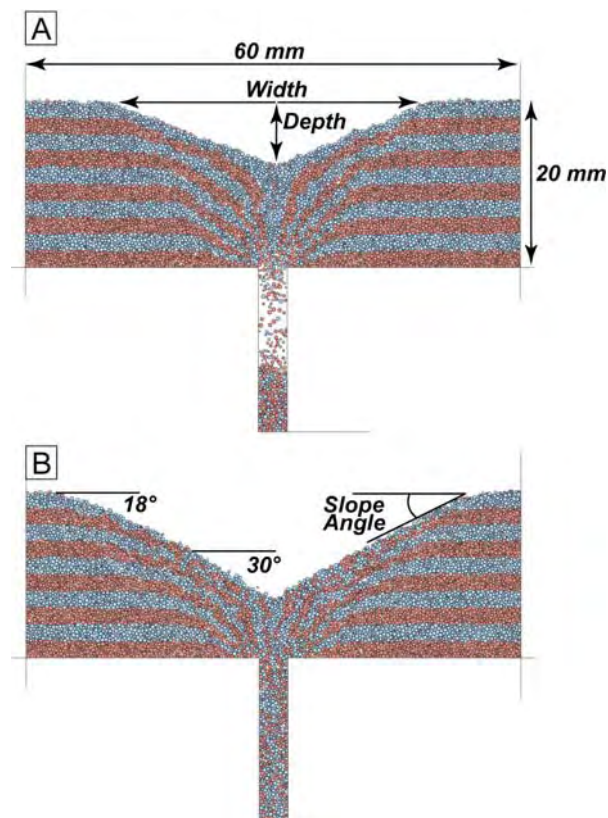


Figure 3. Two-dimensional discrete-element model of pit formation above a vertical extension fracture under Earth's gravitational acceleration. (A) Particle size distribution is randomly generated within the range of 0.09 mm and 0.25 mm. Internal layering in this model is an aid in visualization, but does not introduce material anisotropy. This intermediate stage of pit formation shows pit width and depth and a nearly uniform slope of 21°. (B) Final stage shows an increase in pit width and depth. Slope evolution is more complex with a relatively shallow dip of 18° near the surface to approximately 30° at the base of the pit, similar to results found by [7] for pits on Mars.

Additional constraints on regolith thickness can be obtained using numerical modeling techniques to quantify groove morphology as a function of subsurface material properties and regolith thickness (Fig. 3). The goal is to produce geologically accurate and mechanically valid simulations of groove and pit chain formation processes and to use these calibrated approaches, along with the gravitational acceleration of Eros, to analyze the regolith material properties. Model characteristics such as pit width, depth, and slope angle can then be quantitatively compared to measurements from Eros. Initial models run under Earth's gravitational acceleration have produced complex slope evolution similar to pit crater slopes on Mars [7].

**Discussion:** This work will help to quantify the relationship between the observed distribution of pit chains and grooves and the underlying structure of the subsurface on Eros. The role of the regolith, both in mechanical properties and variation of thickness, likely plays a significant role in the distribution and range of these features. Determining the range of regolith thickness necessary to produce pit chains and grooves that have the widths, depths, and slope angles observed on Eros will provide additional constraints on the spatial distribution of regolith material [11].

**References:** [1] Buczkowski, D.L. et al. (2006) LPSC XXXVII, Abs. [2] Prockter, L. et al. (2002) Icarus, 155, 75-93. [3] Thomas, P.C. et al. (1979) JGR, 84, 8457-8477. [4] Veverka, J. et al. (1994) Icarus, 107, 72-83. [5] Sullivan, R. et al. (1996) Icarus, 120, 119-139. [6] Tanaka, K.L. and Golombek, M.P. (1989) LPSC XIX, Abs. [7] Wyrick, D. et al. (2004) JGR, 10.1029/2004JE002240. [8] Ferrill, D.A. et al. (2004) GSA Today, 14, 10, 4-12. [9] Buczkowski, D.L. et al. (2005) AGU Fall Meeting, Abs. P11A-0098. [10] Thomas P.C. et al. (2001) Nature, 413, 394-396. [11] Thomas P.C. and Robinson M.S. (2005) Nature, 436, 366-369. [12] Thomas, P.C. et al. (2002) Icarus, 155, 18-37.